scientific reports

Check for updates

OPEN

Research on yarn tension control technology for knitting underwear machine based on adaptive ADRC

Laihu Peng[1], Xuyi Xiong[1] & Luojun Wang[1,2]✉

During the operation of the knitting underwear machine, unstable yarn tension can have adverse effects on the quality of the underwear fabric, such as uneven density and reduced resilience, which significantly diminishes the comfort and durability of the textile products. In response to the issues of slow tension response speed and low tension control accuracy in the traditional yarn feeding method of current knitting underwear machines, a tension control system has been designed for the yarn feeding process. The system employs an adaptive ADRC algorithm, which is based on fuzzy sliding mode control, to detect the real-time trend of yarn tension changes, adjust the real-time target speed of the yarn feeding motor, and then utilizes permanent magnet synchronous motor vector control technology to drive the motor operation. This reduces tension disturbances during the yarn feeding process, enhances the response speed during sudden tension changes, and achieves precise control of yarn tension. Finally, a tension controllable yarn feeding experimental platform was constructed to simulate the knitting underwear machine, and tests were conducted to evaluate the control effectiveness of the yarn feeding tension control system under various algorithm controls. The results show that the control system based on the adaptive ADRC algorithm reduces the amplitude of tension fluctuation in the yarn target tension stabilization phase by more than 33% compared to traditional PID and ADRC algorithms. The average response time is shortened by over 35%, respectively. These comparative data demonstrate that the system can enhance the stability of yarn tension control during the yarn feeding process while meeting the varying elasticity demands of different fabrics and the specific yarn feeding speed requirements of various knitting processes, ultimately ensuring fabric quality.

Keywords Knitting underwear machine, Yarn tension control, Adaptive ADRC algorithm, Fuzzy synovial control, Permanent magnet synchronous motor, Yarn feeding control system

As an important textile equipment, the technological characteristics and performance optimization of the knitting underwear machine have been a focal point of both academic and industrial attention. Especially in the weaving process, accurate regulation of yarn tension is regarded as a crucial technical parameter, which not only profoundly affects the structural characteristics of the fabric, but also directly relates to the physical characteristics and quality standards of the final textile. This makes accurate regulation of yarn tension an essential element that urgently requires further exploration and optimization in the textile production process[1,2].

Yarn tension mainly adjusts the appearance and feel of the fabric by influencing two key indicators: fabric resilience and density. Fabric resilience refers to the ability of the fabric to return to its original state after being subjected to external forces, which directly affects the comfort and durability of the textile product[3]. This is primarily controlled by yarn tension. Within a certain range, as yarn tension increases, the yarn generates a greater elastic force to resist deformation, attempting to return to its original shape and size. This suggests that moderate increases in tension can enhance the yarn's elastic properties[4]. Fabric density refers to the number of warp and weft yarns in a unit area. When yarn tension increases, the yarn becomes finer under tensile forces, which reduces its linear density. This allows more yarns to be arranged in the same length of fabric, thereby increasing the fabric's density, which directly impacts the textile's tensile strength and breathability. In conclusion, controlling the stability of yarn tension is an important research topic in the field of textile equipment.

In the field of yarn tension control, researchers are dedicated to enhancing the stability and control precision of the system. On one hand, some scholars focus on the study of yarn tension models and the design of tension

[1]Zhejiang Provincial Key Laboratory of Modern Textile Equipment and Technology, Zhejiang Sci-Tech University, Hangzhou 310018, Zhejiang, China. [2]School of Automation, Zhejiang Polytechnic University of Mechanical and Electrical Engineering, Hangzhou 310053, Zhejiang, China. ✉email: wangluojun@zime.edu.cn

control methods. For instance, Ronggen et al. established an elastic yarn unwinding balloon model and derived the tension variation pattern during the unwinding process, providing a basis for subsequent passive precision tension control devices for elastic fibers[5]. Zhao et al. constructed a tension model based on tension variations during the knitting process of fully-formed weft knitted fabrics and designed a tension compensation device to reduce tension fluctuations and improve fabric quality[6]. Feng et al. designed a carbon fiber warping tension control system, utilizing tension detection equipment in combination with a PLC-controlled servo motor to overcome issues in carbon fiber warping, thereby achieving effective tension control[7].

On the other hand, some scholars have chosen to optimize control algorithms to improve the effectiveness of yarn tension control. Xiao et al. proposed an improved genetic algorithm to optimize the PID control scheme, which compensates for the shortcomings of traditional PID algorithms and enhances the stability of warp yarn tension under various weaving conditions[8]. Li et al. employed a fuzzy multi-attribute group decision-making method to optimize the selection of yarn tension detection and control schemes for shuttle looms, providing new insights for yarn tension control[9]. Wang et al. designed an improved grey prediction method, combined with adaptive PID control, to strengthen control accuracy and anti-jamming capabilities[10]. Zhang Hua et al. applied active disturbance rejection control (ADRC) technology to replace the traditional PID controller in the yarn tension control system, improving the system's robustness[11]. Zheng et al. developed an adaptive yarn tension control system for warp knitting machines using a dual FIFO dynamic interpolation motion method from the perspective of control strategy optimization. This system significantly reduced yarn tension peaks and fluctuations by optimizing control strategies and algorithms[12].

Although these studies have proposed various strategies for yarn tension control, some of which further leverage artificial intelligence algorithms to tune controller parameters and improve system performance, few have focused on improving or optimizing the existing controller algorithms themselves. The limitations of traditional controllers restrict the upper limits of system performance. While Chen et al. introduced a yarn tension sliding mode control strategy based on an extended state observer to improve the dynamic performance of the yarn tension control system[13], they did not consider the complex operational conditions of knitting equipment when different knitting processes are employed. This control strategy may not maintain optimal system robustness and control accuracy under special working conditions.

Based on the fuzzy sliding mode control (FSMC) adaptive ADRC algorithm, this paper designs a yarn tension control system for knitting underwear machines, which is combined with the principle of field-oriented control (FOC) for permanent magnet synchronous motors. The proposed control system uses a fuzzy controller to achieve online self-tuning of sliding mode control parameters. At the same time, it employs a tracking differentiator and an extended state observer (ESO) to enhance the system's ability to suppress unknown disturbances and improve the dynamic control capabilities of the yarn tension feedback loop. This enables dynamic regulation of the yarn tension in the feeder, stabilizes yarn tension fluctuations, reduces yarn breakage and defect rates, and ensures that the fabrics produced by knitting underwear machines are of acceptable quality.

Mechanism of yarn tension formation

High-end lingerie fabrics must provide close-fitting comfort, as well as high elasticity and stability. These requirements impose more stringent control demands on the elastic properties of the yarns during the knitting process. Yarn elasticity is not only influenced by material properties such as the elastic modulus, moisture regain, and breaking strength, but also by the fluctuations in yarn tension that occur during the knitting process, which play a critical role in determining its overall performance[14].

During the operation of knitting underwear machines, yarn tension fluctuations are primarily influenced by three factors: The first point is the variations in the knitting craftsmanship. The starting and stopping of the yarn path, along with changes in fabric density, can cause significant sudden variations in yarn tension. The second point is the environmental conditions during the knitting process. Factors such as temperature, air flow, and the regular pulling motion of the knitting needles can disturb the yarn tension. The third point is the yarn feeding speed. The faster the yarn feeding speed, the more difficult it becomes to control the rotational speed of the feeder, leading to an increase in the frequency of tension fluctuations during yarn movement. If the tension exceeds the yarn's inherent tolerance, it may lead to fabric distortion and yarn breakage, negatively affecting production efficiency. On the other hand, if the tension is too low, the fabric may become loose or shrink. Therefore, maintaining stable yarn tension control in the knitting underwear machine is a critical factor that directly influences the quality of the fabric produced.

The prerequisite for achieving stable yarn tension control is to investigate the mechanism of yarn tension formation during the operation of the knitting underwear machine. As shown in Fig. 1, during the operation of knitting equipment such as the knitting underwear machine, the cylinder rotates at a target speed, denoted as ω_1(r/min), while the feeder motor speed is set to ω_2(r/min). From these parameters, the yarn feed-in speed V_1 (m/s) entering the knitting needles and the yarn feeding speed V_2(m/s) of the feeder can be derived as follows:

$$\begin{aligned} V_1 &= 2\pi r_1 \omega_1 \\ V_2 &= 2\pi r_2 \omega_2 \end{aligned} \tag{1}$$

In the equation,r_1 represents the radius of the needle cylinder (m), and r_2 represents the radius of the yarn storage spool on the yarn feeding device (m).

The yarn tension, denoted as T(N), follows Hooke's law:

$$T = \frac{ES}{l} \int_0^t (V_1 - V_2) dt \tag{2}$$

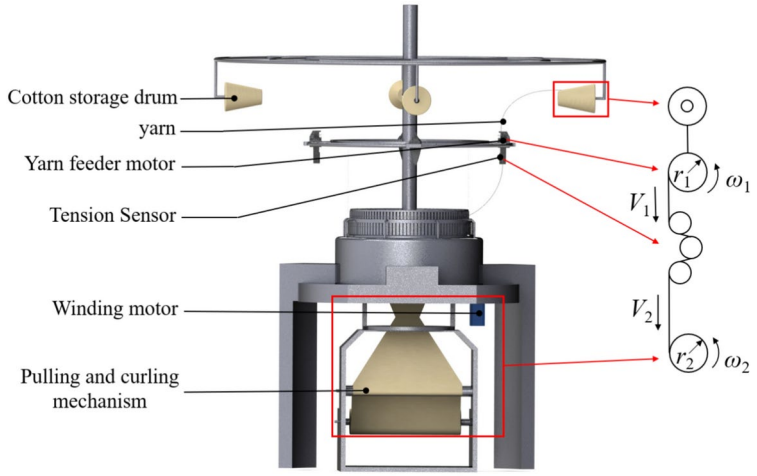

Fig. 1. Model of yarn tension formation mechanism.

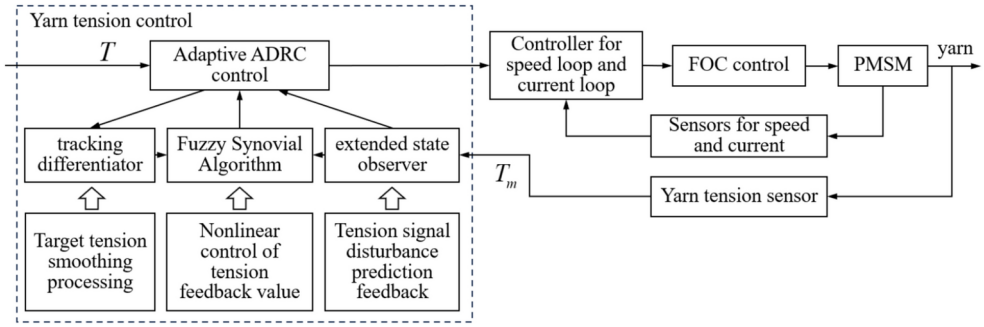

Fig. 2. Framework of the yarn feeding tension control system for knitting underwear machinery.

In the equation, E is the elastic modulus of the yarn (Pa), S is the cross-sectional area of the yarn (m^2), is the elongation of the yarn (m), which is the total length of the yarn from the yarn feeder to the needle cylinder (m).

$$T = 2\pi \frac{ES}{l} \int_0^t (\omega_1 r_1 - \omega_2 r_2) dt \tag{3}$$

The yarn feeder, as an auxiliary feeding device in textile machinery, is one of the few machines capable of actively controlling yarn tension during the operation of the knitting underwear machine. According to Eq. (3), it can be seen that variations in the yarn feeder motor speed directly and sensitively influence the fluctuations in yarn tension. Therefore, achieving precise control of the yarn feeder motor speed, thereby reducing tension fluctuations induced by various influencing factors and ensuring that yarn tension remains within the desired range, is key to improving the robustness of yarn delivery tension control.

Comprehensive design of the yarn delivery control system for the knitting underwear machine

During the operation of the knitting underwear machine, different knitting processes require adjustments to the yarn tension, and maintaining stable tension during the constant tension phase is essential. However, there are still many factors that affect yarn tension. For example, friction between the yarn and the needle hook or old loops during the knitting cycle, the ballooning effect when the yarn unwinds from the yarn cone, and variations in the cylinder speed of the knitting machine can all disturb the yarn tension. To suppress yarn tension fluctuations and ensure stability during the feeding process, an appropriate controller can be designed to minimize the impact of external disturbances, while also adjusting the rotational speed of the PMSM (Permanent Magnet Synchronous Motor), thereby achieving stable control of yarn tension.

The overall framework of the yarn feeding tension control system for the knitting underwear machine is shown in Fig. 2. The system takes the target yarn tension T as the input, which is processed for smoothing through the tracking differentiator. The real-time yarn tension T_m serves as the negative feedback signal. The adaptive ADRC (active disturbance rejection control) controller utilizes the extended state observer (ESO) to predict and provide feedback on disturbances in the real-time tension signal. Finally, the fuzzy sliding mode

algorithm is applied for the nonlinear control of the feedback signal, enabling the adjustment of the target rotational speed of the PMSM. The FOC technology is then used to complete the closed-loop control of the PMSM, thereby constructing the yarn feeding tension control system for the knitting underwear machine.

The design of yarn tension control

As shown in Fig. 2, the structure of the adaptive ADRC controller consists of a tracking differentiator (TD), an extended state observer (ESO), and a fuzzy sliding mode controller (FSMC). These components are responsible for the smoothing of the target yarn tension, prediction feedback of tension signal disturbances, and nonlinear control of the tension feedback value, respectively. The detailed structure is illustrated in Fig. 3.

The adaptive ADRC controller first smooths the target yarn tension signal T using the TD. The smoothed target tension signal T_1 and its derivative T_2 are then passed to the FSMC, which processes them to generate the adjustment signal ΔA for the PMSM speed. This signal, along with the reference speed signal ω_{ref} for the yarn feeding motor, is sent to the vector control section of the yarn feeding motor[15]. Simultaneously, the encoder of the PMSM provides real-time motor speed ω_m feedback to the vector control section, thereby completing the closed-loop control.

Additionally, the tension sensor feeds the actual yarn tension signal T_m back to the ESO of the adaptive ADRC controller. The ESO uses this feedback signal to estimate disturbances in the yarn tension control system. z_1 represents the observed yarn tension output, z_2 is the derivative of the yarn tension observation, and z_3 is the predicted total disturbance of the yarn tension control system. The ESO compensates for disturbances in T_1, T_2, and ΔA to improve the controller's dynamic performance and robustness, ensuring a stable output signal[16].

Smooth processing mechanism for target value of yarn tension

To address the issue of sudden changes in yarn tension caused by variations in the knitting process, the adaptive ADRC controller uses a tracking differentiator to smooth the tension target values that undergo abrupt changes during the start-stop phase of the yarn path and the fabric density adjustment phase. A low-pass filter is applied to reduce signal overshoot and mitigate noise amplification effects. Meanwhile, the differentiation stage outputs the derivative of the smoothed signal, thereby improving the abrupt changes and overshoot phenomena of the controller's output signal under varying knitting process[17].

The TD will output T_1 and T_2, and the discrete system formula is as follows:

$$\begin{cases} T_1(k+1) = T_1(k) + h \cdot T_2(k) \\ T_2(k+1) = T_2(k) + h \cdot \text{fhan}\left(T_1(k) - T, T_2(k), r, h\right) \end{cases} \tag{4}$$

In the equation, k represents the sampling time; T is the system initial value; h is the integration step size; r is the speed factor; and the fhan function is the fastest synthesis function, which is used to rapidly track the tension signal while avoiding the interference of steady-state oscillations.

The equation for the fhan function is as follows:

$$\begin{cases} d = rh^2 \\ a_0 = hx_2 \\ y = x_1 + a_0 \\ a_1 = \sqrt{d(d + 8|y|)} \\ a_2 = a_0 + \text{sign}(y)\left(a_1 - d\right)/2 \\ a = (a_0 + y)\,\text{fsg}(a, d) - r\text{sign}(a)(1 - \text{fsg}(a, d)) \\ \text{fhan} = -r\left(\frac{a}{d}\right) - r\text{sign}(a)(1 - \text{fsg}(a, d)) \end{cases} \tag{5}$$

In the equation, sign() is the sign function. The fsg function is as follows:

$$\text{fsg}(x, y) = (\text{sign}(x + y) - \text{sign}(x - y))/2 \tag{6}$$

When the target tension signal of the yarn experiences a sudden change, the TD will smooth it out to reduce the noise amplification effect and stabilize the target tension signal of the yarn.

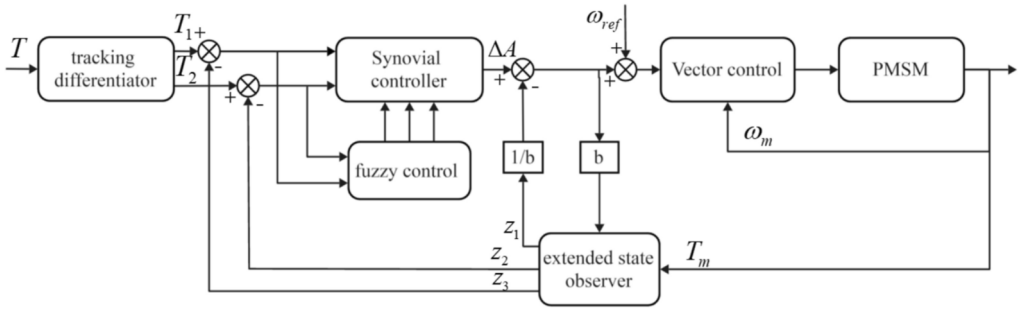

Fig. 3. Adaptive ADRC controller structure.

Prediction mechanism of yarn tension signal disturbance

Due to the influence of various environmental factors, the pulling force exerted by the knitting needles on the yarn, and the vibrations of the sensor itself during yarn transport, the real-time tension signal of the yarn is subject to high-frequency signal noise and significant disturbances. The adaptive ADRC controller uses the ESO to track the actual yarn tension signal. By treating the uncertainties and external disturbances in the yarn tension control system as extended states, the ESO estimates and predicts the overall system state using input signal Tm and output signals z_1, z_2, z_3. This allows the identification of the total external disturbance and, consequently, the calculation of the system's disturbance compensation using the control function, thus reducing the impact of disturbances on the system and improving the control performance.

The discrete system formula for the second-order system Extended State Observer can be expressed as:

$$\begin{cases} e = z_1(k) - y(k) \\ z_1(k+1) = z_1(k) + h\left(z_2(k) - \beta_1 e\right) \\ z_2(k+1) = z_2(k) + h\left(z_3(k) - \beta_2 \mathrm{fal}\left(e, \alpha_1, \delta\right)\right) + b \cdot u \\ z_3(k+1) = z_3(k) - h \cdot \beta_3 \mathrm{fal}\left(e, \alpha_2, \delta\right) \end{cases} \tag{7}$$

In the equation: β_1, β_2, and β_3 are observation coefficients, where β_1 affects the lag in the estimation of system disturbance, while β_2 and β_3 influence the degree of system oscillation. The formula for the fal function is as follows:

$$\mathrm{fal}(e, \alpha, \delta) = \begin{cases} \frac{e}{\delta^{1-\alpha}}, |e| \le \delta \\ |e|^{\alpha}\mathrm{sign}(e), |e| > \delta \end{cases} \tag{8}$$

In the equation: e represents the estimation error of the output by the ESO, α is a constant ($0 < \alpha < 1$), and b is a filtering parameter ($\delta > 0$). When $\alpha < 1$, the fal function exhibits the characteristic of "small error, large gain; large error, small gain," which can improve prediction performance.

Nonlinear control of yarn tension feedback signal

The yarn elasticity model exhibits various nonlinear characteristics, such as stress–strain relationships, friction variations, and dynamic vibrations. These nonlinearities arise from the inherent physical properties of the yarn material and the complex interactions occurring during the knitting process. They change nonlinearly with factors such as yarn stress, deformation, and speed. As a result, traditional controllers struggle to meet the current demands of textile production, as their performance is limited by linear combinations and they lack adaptive regulation capabilities.

The adaptive ADRC controller utilizes a fuzzy sliding mode controller as the nonlinear control law, allowing it to dynamically adjust the tension control strategy based on real-time feedback to cope with rapid changes in yarn tension and complex disturbances[18,19]. First, the system state model is constructed using a sliding mode function, processing the output signals from the tracking differentiator and the extended state observer. Meanwhile, the fuzzy controller adjusts the sliding mode algorithm parameters based on the input parameters, achieving adaptive control and improving both control accuracy and stability[20,21].

The state variables of the PMSM tension control system are defined as follows:

$$\begin{cases} x_1 = T_{\mathrm{ref}} - T_m \\ x_2 = \dot{x}_1 = -\dot{T}_m \end{cases} \tag{9}$$

In the equation, T_{ref} represents the target parameter of yarn tension after smoothing by the TD. T_m represents the observed output of yarn tension, which is the actual value of yarn tension after observation and analysis.

Based on the mathematical model of the yarn tension control system, the sliding surface s is designed as follows:

$$s = c\mathrm{x}_1 + \mathrm{x}_2 \tag{10}$$

In the equation, c is an undetermined parameter with the condition that $c > 0$.

From Eq. (3), it is evident that yarn tension is determined by the difference in rotational speeds between the needle cylinder and the yarn feeder. Since the rotational speed of the needle cylinder is constant, yarn tension is directly controlled by adjusting the rotational speed of the yarn feeder motor. For clarity, a variable ΔA is introduced, which represents the influence of the target tension on the rotational speed of the yarn feeder motor.

Since:

$$\lim_{t\to\infty} \omega_1 r_1 = \lim_{t\to\infty} \omega_2 r_2 = C \tag{11}$$

In the equation, C is a constant, let $\omega_2 r_2 = \left(\omega_1 \frac{r_1}{r_2} - \Delta A\right) \cdot r_2$, where $\lim_{t\to\infty} \Delta A = 0$ 。

Therefore, by combining formula 6, we can obtain:

$$\begin{cases} \dot{x}_1 = -\dot{T}_m = -2\pi \frac{ES}{l} \cdot r_2 \cdot \Delta A \\ \dot{x}_2 = -\ddot{T}_m = -2\pi \frac{ES}{l} \cdot r_2 \cdot \Delta \dot{A} \end{cases} \tag{12}$$

For convenience in calculation, let $u = \frac{d\Delta A}{dt}$ and $D = \frac{2\pi ES \cdot r_2}{l}$. The derivative of the sliding surface function can be obtained as follows:

$$\dot{s} = c\dot{x}_1 + \dot{x}_2 = cx_2 + \dot{x}_2 = cx_2 - Du \tag{13}$$

Adopting the variable exponential reaching rate::

$$\begin{cases} \dot{s} = -\varepsilon |x_1| \operatorname{sgn}(s) - ps \\ \lim\limits_{t \to \infty} |x_1| = 0 \end{cases} \tag{14}$$

In the equation: ε and p are positive numbers, and $0 < \varepsilon < p$. The controller expression can be obtained from Eq. 14.

$$u = \frac{1}{D} [cx_2 + \varepsilon |x_1| \operatorname{sgn}(s) + ps] \tag{15}$$

The influence of yarn target tension on yarn feeder motor rotational speed can be expressed as:

$$\Delta A = \frac{1}{D} \int_0^t [cx_2 + \varepsilon |x_1| \operatorname{sgn}(s) + ps] \mathrm{d}t \tag{16}$$

To prove the asymptotic stability of the fuzzy sliding mode controller, a Lyapunov function is selected:

$$V = \frac{1}{2} s^2 \tag{17}$$

According to the Lyapunov stability condition, the stability condition of the controller needs to meet $\dot{V} = s\dot{s} \leq 0$ [22,23]. From the combination of formula 14 and formula 17:

$$s\dot{s} = s(-\varepsilon |x_1| \operatorname{sgn}(s) - ps) = -\varepsilon s |x_1| \operatorname{sgn}(s) - ps^2 \tag{18}$$

It is evident that when $s > 0$, $s\dot{s} < 0$, and when $s < 0$, $s\dot{s} > 0$. This shows that the reaching law satisfies the sliding mode reaching condition, enabling the system to enter the sliding state[24,25].

The fuzzy controller adopts a two-input and three-output configuration. The basic universe of discourse for the input variable E (error) is (− 20, 20), and for EC (error change) it is (− 300, 300). The basic universes of discourse for the output variables c,p and ε are (− 0.2, 0.2), (− 1, 1) and (− 0.3, 0.3), respectively. The fuzzy subsets for each variable of the fuzzy controller are {NB, NM, NS, ZE, PS, PM, PB}, denoted as {NB, NM, NS, ZE, PS, PM, PB}. Furthermore, a fuzzy rule table is formulated based on the input parameters T_1 and T_2 to set the adaptive change conditions and ranges for the controller parameters c,p and ε. This helps to reduce system chattering, thereby enhancing the dynamic performance and robustness of the controller and providing a stable output signal[26,27].

Hardware design of yarn tension control

The hardware control design of the yarn feeding device is shown in Fig. 4. The system hardware control structure mainly consists of the main control chip STM32F405RGT6, yarn tension operational amplifier circuit, three-phase inverter circuit, Hall differential operational amplifier circuit, and three-phase current sampling circuit. In the system control program, the tension loop controller, based on the adaptive ADRC algorithm, is combined with FOC technology to achieve the tension control of the yarn feeding device.

The tension control signal set by the main control chip is first transmitted to the tension loop controller, where the signal is processed by the adaptive ADRC algorithm. The tracking differentiator smooths the input

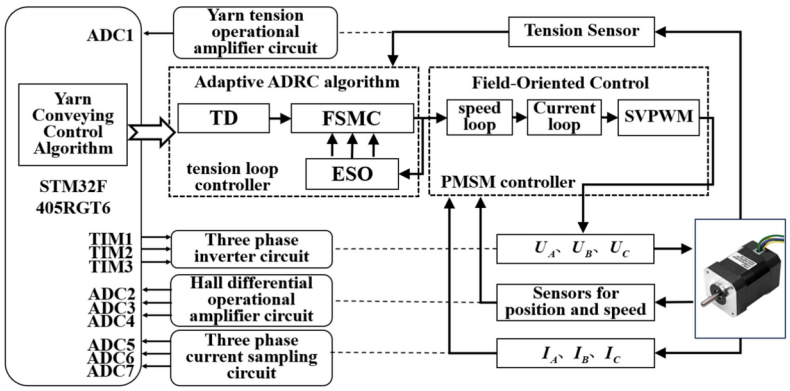

Fig. 4. The block diagram of the system control hardware design.

signal to reduce the impact of signal fluctuations and sudden changes. The role of the FSMC(fuzzy sliding mode control algorithm) is to transform the input signal into a speed control signal, while simultaneously mitigating signal oscillations and accelerating the response time. The expansion state observer collects the output signal of the tension loop controller and the real-time yarn tension signal, estimates system disturbances, and outputs a compensation signal to feedback regulate the fuzzy sliding mode algorithm[28,29]. Subsequently, the permanent magnet synchronous motor controller processes the speed control signal through the speed loop, current loop, and space vector pulse width modulation (SVPWM), generating three-phase control voltages U_A, U_B, U_C, which are then used to drive the permanent magnet synchronous motor through the three-phase inverter circuit.

Finally, the three-phase current sampling circuit and the position and speed sensors will feedback the three-phase current signals I_A, I_B, I_C, as well as the motor rotor speed and angle signals, to the permanent magnet synchronous motor controller. This enables real-time adjustment of the motor rotational speed and control current. Meanwhile, the real-time yarn tension signal is fed back to the tension loop controller via the tension sensor, completing the closed-loop control of the yarn tension by the yarn feeding system[30].

Simulation of yarn feeding control system for knitting underwear machine

Simulation environment construction

In this section, a simulation model of the yarn feeding tension control system was built using simulation software. Two important indicators of textile quality, namely fabric resilience and fabric density, were simulated. Two working conditions were simulated: one involves the periodic switching of different elastic requirements for the fabric during the weaving process, while the other involves the adjustment of yarn feeding speed under different knitting processes.

The yarn tension during the operation of the knitting underwear machine is generally controlled within 20% of the yarn fracture force. Based on the fineness range of commonly used yarns for underwear weaving (such as 14-18tex for cotton yarn and 4.4–7.7tex for spandex core spun yarn) and the fracture strength range (such as 7-15cN/tex for cotton yarn and 14-25cN/tex for spandex core spun yarn), the yarn tension control range is determined to be 0-55cN. Therefore, this range is set as the target tension value for simulation experiments. In addition, simulation experiments were conducted based on real knitting conditions of the underwear machine, and the needle cylinder speed during the underwear fabric weaving process was set within 60–120 r/min (data sourced from SANTONI TOP2-FAST 22 inch seamless knitting underwear machine).

Other simulation settings are as follows: bus voltage is set to 24 V, PWM switching frequency is set to 12 kHz, sampling period is set to 1e−5 s, and the simulation duration is set to 10 s. Simultaneously select a random signal generation module to add to the system simulation model, with an interference interval of 1e−4 s, to simulate the environmental interference signals under the operation of the yarn feeding tension control system. The simulation model of the yarn feeding tension control system is shown in Fig. 5. The relevant parameters of the PMSM motor in the simulation model are derived from the actual parameters of the yarn feeder motor listed in Table 1.

Performance analysis of yarn under varying target tensions

In the simulation experiment of the periodic variation of the yarn target tension, the initial rotational speed of the needle cylinder is set to 80 r/min (corresponding to the yarn feeder motor rotational speed of 2000 r/min). The input signal for the yarn target tension is a square wave with a frequency of 3 Hz, a duty cycle of 50%, a peak value of 35 cN, and a trough value of 15 cN. The experimental results present a subset of the simulation data over a duration of 2 s, as shown in Figs. 6 and 7.

Figure 6 shows the tension variation curve under the periodic change of the yarn target tension. According to Tables 2 and 3. During the sharp decrease of the target tension, the tension curve under the control of the adaptive ADRC algorithm exhibits the smallest absolute maximum deviation and the shortest response time, reducing by 73.1% and 45.3%, respectively, compared to the PID control algorithm. When compared to the ADRC control algorithm, the reduction is 56.7% and 39.6%, respectively. In the phase of sharp increase in the target tension, the adaptive ADRC algorithm reduces the maximum deviation of the tension curve by more than half compared to the other two algorithms, and the response time is shortened by more than 1/4, the control of overshoot is better than that of the other two algorithms.

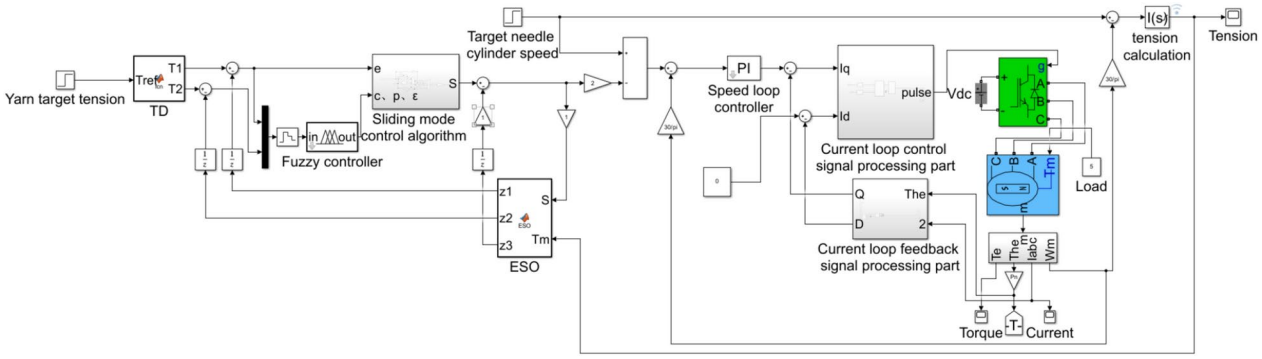

Fig. 5. Simulation model of yarn conveyor tension control system.

Parameter	Parameter values
Rated torque T_L/(N·m)	0.18
Rotor magnetic flux ψ_f/Wb	0.175
Stator resistance R_s/Ω	2.875
Direct axis inductance L_d/H	8.5×10^{-3}
Quadrature axis inductance L_q/H	8.5×10^{-3}
Moment of inertia J/(kg·m^2)	0.008
number of pole pairs P_n/pair	4

Table 1. Relevant parameters of the simulation model for permanent magnet synchronous motor.

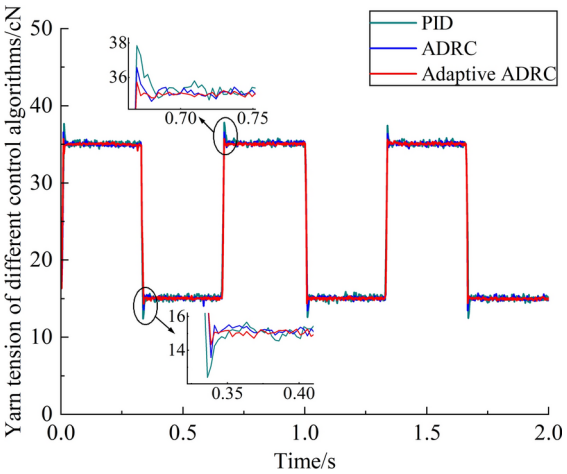

Fig. 6. Simulation curves of yarn tension under varying target tension.

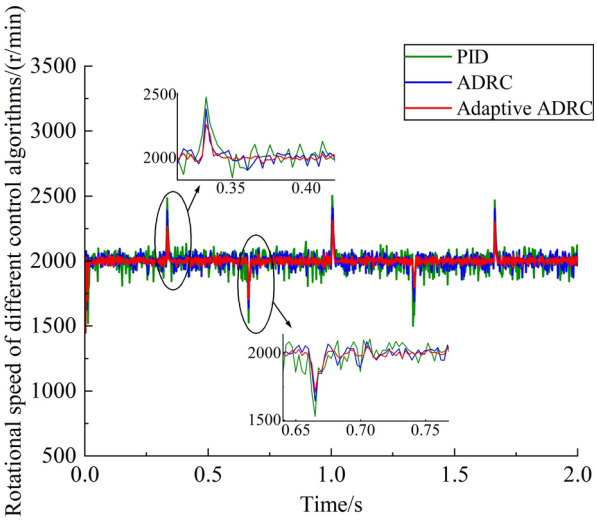

Fig. 7. Simulation curves of yarn feeder rotational speed under varying target tension.

	PID		ADRC		Adaptive ADRC	
Tension stabilization phase	Mean error/cN	Standard deviation/cN	Mean error/cN	Standard deviation/cN	Mean error/cN	Standard deviation/cN
15cN	0.102	0.289	0.062	0.192	0.025	0.124
35cN	0.111	0.276	0.064	0.206	0.025	0.126

Table 2. Tension simulation results of different algorithms in tension stabilization phase.

Tension fluctuation phase	PID		ADRC		Adaptive ADRC	
	Maximum deviation /cN	Response time /s	Maximum deviation /cN	Response time /s	Maximum deviation /cN	Response time /s
15cN-35cN	2.75	0.0223	1.58	0.0173	0.73	0.0123
35cN-15cN	− 2.42	0.0201	− 1.50	0.0182	− 0.65	0.0110

Table 3. Tension simulation results of different algorithms in tension fluctuation phase.

Speed fluctuation phase	Target tension increased by 20cN		Target tension reduced by 20cN	
	Undershoot/(r/min)	Response time/s	Overshoot/(r/min)	Response time/s
PID	476.2	0.0209	504.9	0.0193
ADRC	391.1	0.0174	374.4	0.0169
Adaptive ADRC	298.3	0.0117	315.5	0.0111

Table 4. Simulation results of motor rotational speed for different algorithms under varying target tensions.

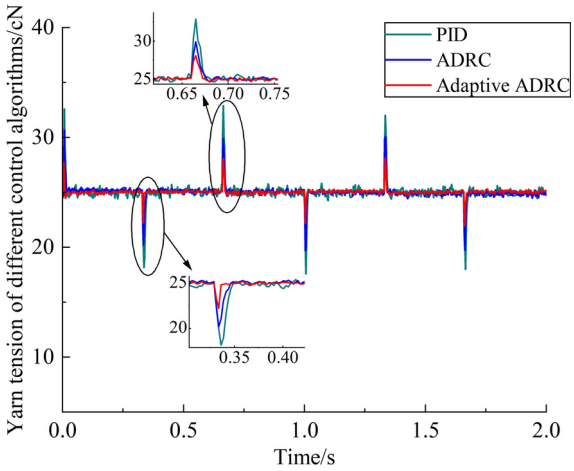

Fig. 8. Simulation curves of yarn tension under target rotational speed adjustment of needle cylinder.

Figure 7 shows the motor rotational speed variation curve under the periodic change of yarn tension. In Fig. 7, when the yarn target tension changes, the motor rotational speed corresponding to all three control algorithms experiences instantaneous fluctuations, and the fluctuation trend of the motor rotational speed is opposite to the variation trend of the target tension, which is consistent with the relationship described in Eq. 6. According to the data in Table 4, the response time of the motor rotational speed fluctuation stage under each algorithm differs from the response time of the corresponding tension fluctuation stage by less than 7%, indicating that the motor rotational speed variation is synchronized with the yarn tension change, thus confirming the direct relationship between the two in the yarn tension formation mechanism. The overshoot and undershoot of the motor rotational speed fluctuations under the adaptive ADRC algorithm are the smallest, with a response time shortened by more than 30% compared to the other two algorithms. This demonstrates that the adaptive ADRC algorithm improves the yarn tension control performance by better regulating the motor speed, thereby better meeting the varying elasticity requirements of different types of fabrics.

Performance analysis of needle cylinder under varying target rotational speed

In the simulation experiment of dynamic adjustment of the needle cylinder's target rotational speed, the needle cylinder motor starts from rest, with the initial yarn tension set to 25 cN. The input signal for the needle cylinder's target rotational speed is a square wave with a frequency of 3 Hz, a duty cycle of 50%, a peak value of 100 r/min, and a valley value of 60 r/min (corresponding to a peak speed of 2500 r/min and a valley speed of 1500 r/min for the yarn feeder motor). The experimental results are extracted from 2-s simulation data, and the data images are presented in Figs. 8 and 9.

Figure 8 illustrates the real-time rotational speed curves of the yarn feeder under dynamic adjustment of the needle cylinder target speed for different control algorithms. According to the data in Tables 5 and 6, compared to the traditional PID algorithm, the absolute value of the mean error during the steady-state phase of the rotational speed for the adaptive ADRC algorithm curve is reduced by approximately two-thirds. The standard deviation is shortened by more than half compared to both the PID algorithm and the ADRC algorithm. During the rotational speed fluctuation phase, the adaptive ADRC algorithm curve exhibits the smallest maximum

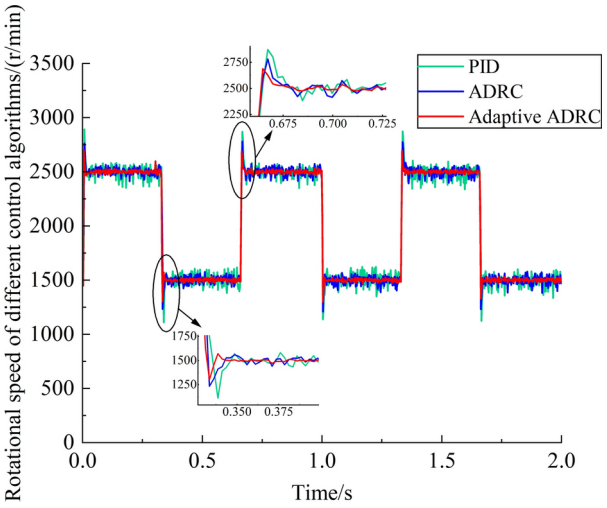

Fig. 9. Simulation curves of yarn feeder rotational speed under target rotational speed adjustment of needle cylinder.

	PID		ADRC		Adaptive ADRC	
Speed stabilization phase	Mean error/cN	Standard deviation/cN	Mean error/cN	Standard deviation/cN	Mean error /cN	Standard deviation/cN
1500r/min	1.33	54.8	0.712	36.8	0.446	13.4
2500r/min	− 1.42	51.3	− 0.762	36.7	− 0.453	14.7

Table 5. Simulation results of yarn feeder rotational speed for different algorithms in rotational speed stabilization phase.

	PID		ADRC		Adaptive ADRC	
Speed fluctuation phase	Maximum deviation/(r/min)	Response time/s	Maximum deviation/(r/min)	Response time/s	Maximum deviation/(r/min)	Response time/s
1500r/min–2500r/min	382	0.0167	272	0.0131	192	0.0099
2500r/min–1500r/min	− 376	0.0173	− 278	0.0124	− 190	0.0094

Table 6. Simulation results of yarn feeder rotational speed for different algorithms in rotational speed fluctuation phase.

	Rotational speed of needle cylinder is increased by 40r/min		Rotational speed of needle cylinder isreduced by 40r/min	
Tension fluctuation phase	Overshoot/cN	Response time /s	Undershoot/cN	Response time /s
PID	7.48	0.0161	7.10	0.0154
ADRC	5.25	0.0136	5.13	0.0127
Adaptive ADRC	2.98	0.0107	2.88	0.0105

Table 7. Tension simulation results of different algorithms under varying needle cylinder rotational speed.

deviation in rotational speed, with reductions of 49.6% and 30.7% compared to the PID and ADRC control algorithms, respectively, and the response time is controlled within 0.01 s.

Figure 9 presents the rotational speed variation curves of the yarn feeder for different control algorithms under dynamic adjustment of the needle cylinder target rotational speed. As indicated in Table 7, during the tension fluctuation phase, under varying conditions of the needle cylinder target speed changes, the three algorithms show relatively small differences in tension variation and response time. Among them, the overshoot and undershoot of the adaptive ADRC algorithm curve are significantly lower than the other two algorithms, with a maximum value of only 2.98cN. Its average response time is 0.0106 s, representing a reduction of 32.7% and 19.4% compared to the PID algorithm and the ADRC algorithm, respectively. Taken together, the adaptive ADRC algorithm maintains superior control performance during dynamic adjustment of the needle cylinder target rotational speed, while also accommodating real-time yarn tension regulation. This demonstrates that the

algorithm can better meet the rotational speed requirements of knitting underwear machines under different knitting processes.

Verification and analysis of yarn feeding experiment

Construction of experimental platform

To practically verify the tension control performance of the yarn feeding control system, which combines the tension controller optimized by the adaptive ADRC algorithm with the vector-controlled permanent magnet synchronous motor, and to assess whether it can meet the varying elastic demands of different fabric weaving processes and the corresponding speed requirements for knitting underwear machines in various knitting techniques. Based on the operating model structure of the yarn feeder and knitting underwear machine, a controllable tension yarn feeding experimental platform was built, as shown in Fig. 10.

The experimental platform utilizes a winder motor to drive the yarn drum to rotate at a specified speed, while employing a yarn guide mechanism with a translating guide track to guide the yarn to swing left and right, ensuring the yarn is wound on the drum in a regular pattern.

The cotton yarn used in high-quality fabrics serves as the primary experimental subject. The yarn feeding experimental platform primarily consists of a yarn storage cylinder, a controllable tension yarn feeder, a yarn guide hole translation guide rail, a yarn winding cylinder, a winding motor (simulating the needle cylinder of a knitting underwear machine), and an upper computer. The tension sensor in the controlled tension yarn feeder collects real-time tension data of the yarn at a sampling frequency of 100 Hz and uploads it to the Serial Plot software on the host computer for display, allowing for the observation of real-time tension variations during the yarn feeding process.

Verification of yarn feeder control performance

To validate the simulation results presented in Sections "Prediction mechanism of yarn tension signal disturbance" and "Nonlinear control of yarn tension feedback signal", a controlled tension yarn feeding experimental platform was utilized to periodically adjust both the target tension value of the yarn feeder and the simulated motor speed of the needle cylinder. Physical experiments were conducted to compare and verify the tension control effectiveness of different control algorithms in these two distinct environments when applied to the yarn feeding system. Additionally, the study examined whether the adaptive ADRC algorithm controller retains its advantages over other algorithm controllers under various yarn types.

Verification experiment of periodic adjustment of yarn target tension

To verify the yarn feeding system's control effectiveness under varying yarn target tensions, the initial value of yarn target tension is set at 30cN, and the initial rotational speed of the needle cylinder simulation motor is set at 102r/min (corresponding to a yarn feeder rotational speed of 2550r/min). In the experiment, the operations of reducing and increasing the target tension by 20 cN were carried out sequentially at 5-s intervals, resulting in a total of three changes in target tension, accumulatively changing the yarn target tension 3 times. The real-time tension change curves for each algorithm in this set of experiments are shown in Fig. 11, and the tension data is presented in Tables 8 and 9. Figure 12 presents the statistical results of the average maximum deviation of tension, average standard deviation of tension, and average response time for controllers based on different algorithms, obtained by repeating the aforementioned experiments 200 times.

In the first stage of increasing yarn tension (0–5 s), the sudden change in yarn speed and the movement of the yarn guide rail will cause the yarn to undergo a brief oscillation before reaching a steady operating state. During this process, the real-time yarn tension will sharply increase, accompanied by significant oscillations, before stabilizing, resulting in a notable overshoot phenomenon. In this stage, the overshoot peak of the tension curve for the adaptive ADRC algorithm reaches 39.97 cN, which is 3.82 cN and 9.38 cN lower than the peak values of the PID and ADRC algorithms, respectively. The adaptive ADRC algorithm achieves the shortest response time of 0.98 s, which is 52% and 40.9% faster than PID algorithm and ADRC algorithm, respectively. These results demonstrate that the adaptive ADRC algorithm offers superior control performance in mitigating overshoot phenomena.

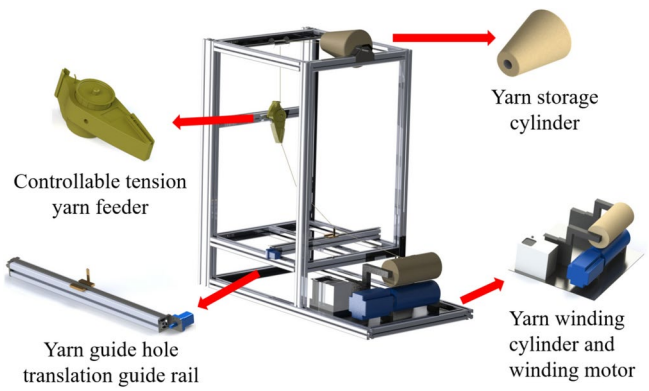

Fig. 10. Model diagram of experimental platform.

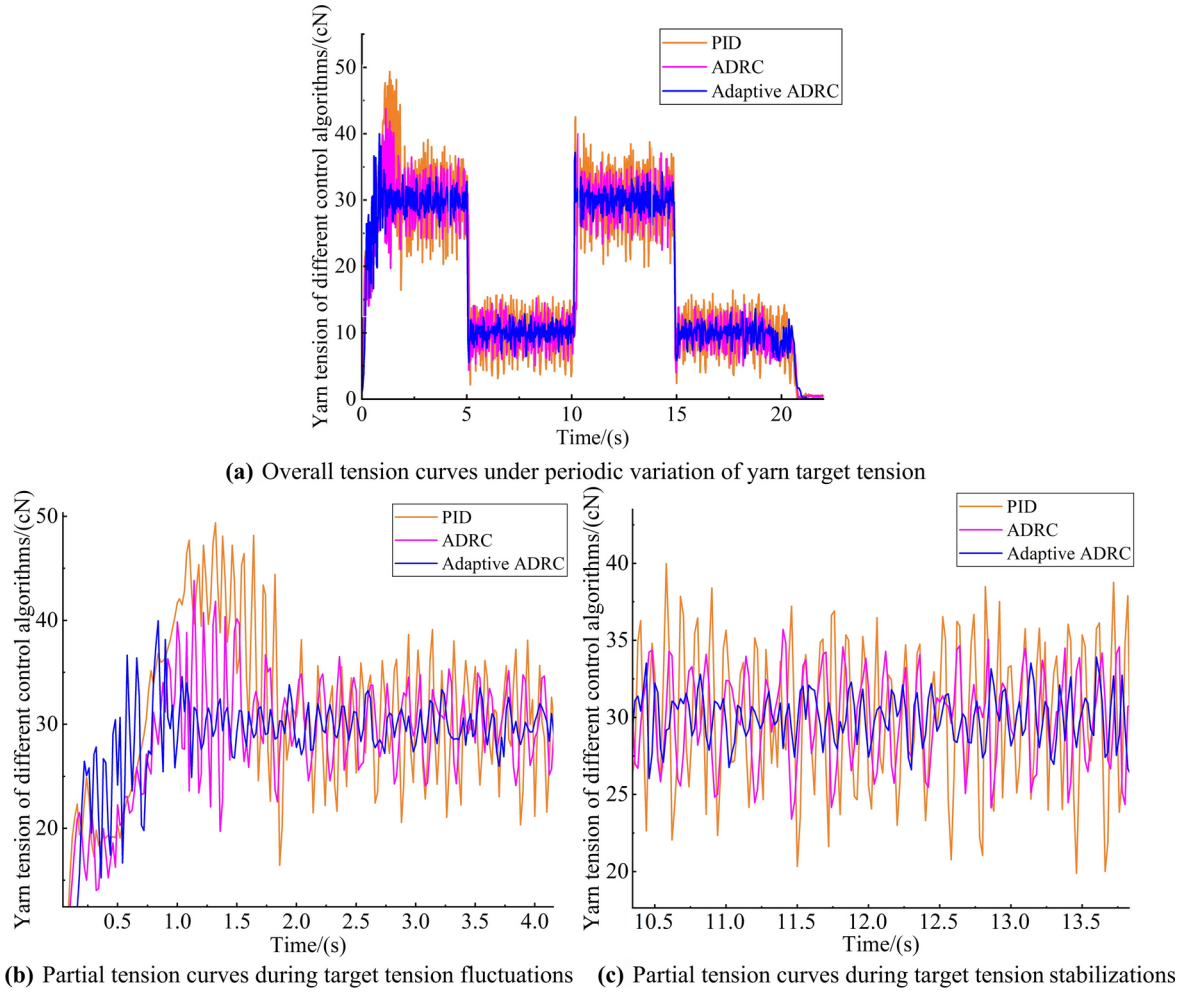

Fig. 11. Overall results of the target tension periodic variation experiment.

Tension stabilization phase	PID		ADRC		Adaptive ADRC	
	Mean error/cN	Standard deviation/cN	Mean error/cN	Standard deviation/cN	Mean error/cN	Standard deviation/cN
30cN	0.28	4.26	0.19	3.27	0.066	1.70
10cN	0.12	2.94	0.089	2.18	0.038	1.37

Table 8. Tension results of stabilization phase under periodic variations of yarn target tension.

Tension fluctuation phase	Target tension increases by 20cN		Target tension reduces by 20cN	
	Overshoot/cN	Response time/s	Undershoot/cN	Response time/s
PID	12.60	0.94	7.74	0.69
ADRC	9.98	0.62	5.79	0.48
Adaptive ADRC	7.20	0.47	4.13	0.24

Table 9. Tension results of fluctuation phase under periodic variations of yarn target tension.

In the steady-state portion of the tension, compared to the other two control algorithms, the tension curve controlled by the adaptive ADRC algorithm exhibits smaller fluctuations at each steady stage. The average mean error is the lowest, at only 0.052 cN, and the average standard deviation is 1.54 cN, which represents an improvement of over 40% compared to the PID and ADRC algorithms. Additionally, during transitions in the yarn target tension, the adaptive ADRC algorithm exhibits the shortest average response time, optimizing the response by 57.6% and 37.1% over the PID and ADRC algorithms, respectively. These improvements align

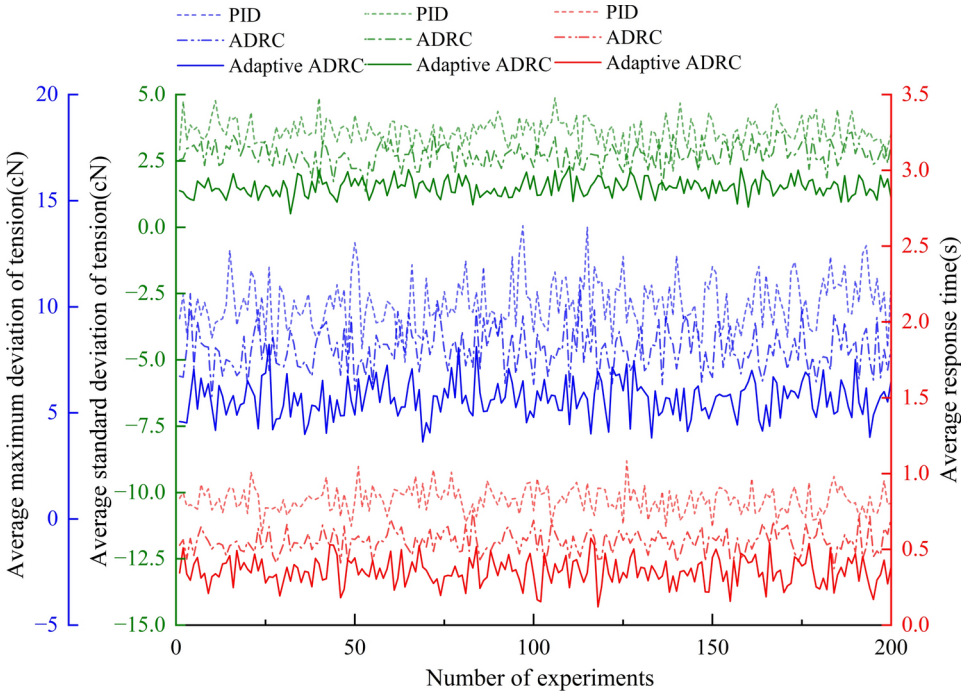

Fig. 12. Experimental results of various performance indexes of different algorithms in multiple rounds of variable target tension experiment.

with the results from the yarn target tension periodic change simulation experiments, confirming that the adaptive ADRC control algorithm exhibits stronger disturbance rejection capabilities compared to the other two algorithms.

Furthermore, a statistical analysis of the experimental data for the three control algorithms in Fig. 12, conducted at a 95% confidence level, reveals that the adaptive ADRC algorithm significantly outperforms both the PID and ADRC algorithms in terms of tension control precision and response speed. Specifically, the 95% confidence interval for the mean standard deviation of yarn tension under the adaptive ADRC algorithm is [1.48, 1.56]cN, which represents a 57.8% reduction compared to the interval of [3.53, 3.65]cN for the PID algorithm and a 44.6% reduction compared to the interval of [2.69, 2.79]cN for the ADRC algorithm. This demonstrates a substantial enhancement in tension control accuracy. Additionally, the confidence interval for the mean response time of the adaptive ADRC algorithm is [0.345, 0.365] seconds, which is 56.7% faster than the response time of the PID algorithm and 35.4% faster than that of the ADRC algorithm. These results collectively validate the superior dynamic response and control precision of the adaptive ADRC algorithm.

Verification experiment for periodic adjustment of target rotational speed of needle cylinder

To validate the performance of the yarn feeding system under variations in the needle cylinder's target rotational speed, the initial rotational speed of the needle cylinder's simulation motor is set to 119 r/min (corresponding to a yarn feeding motor speed of 2975 r/min). Subsequently, the target rotational speed of the needle cylinder's motor is sequentially adjusted every 5 s, in turn, to 51 r/min, 119 r/min, and 51 r/min. Each rotational speed change requires 1 s for acceleration or deceleration (each rotational speed stage consists of 1 s for acceleration/deceleration and 4 s for steady-state operation). The target yarn tension is set to 25 cN. The motor rotational speed curve for the yarn feeder in this experiment is shown in Fig. 13a, while the tension variation curves for each algorithm are shown in Fig. 13b. The tension data is presented in Tables 10 and 11. Figure 14 showcases the statistical outcomes of the average maximum deviation in tension, the average standard deviation of tension, and the average response time for controllers employing various algorithms, derived from repeating the aforementioned experiments 200 times.

In Figs. 13a and 12b, during the acceleration or deceleration phases of the needle cylinder's simulation motor (0-1 s, 5-6 s, 10-11 s, 15-16 s), except for the first acceleration-deceleration phase, the real-time tension exhibits the same trend as the motor rotational speed variation in the subsequent phases. According to Tables 10 and 11. The tension curve of the adaptive ADRC algorithm outperforms the other two algorithms in terms of control precision, with an average maximum deviation of 22.3% and an average standard deviation of 1.53 cN. Additionally, the average response time is reduced by 55.2% and 35.3% compared to the PID and ADRC algorithms. These results are consistent with the trend observed in the rotational speed mutation phases shown in Fig. 7, confirming that the adaptive ADRC algorithm has the characteristics of lower overshoot and faster steady-state recovery compared to the PID and ADRC algorithms. This shows that the system can improve yarn tension control accuracy and response speed, strengthen fabric resilience, reduce density inequality defects, and optimize product quality.

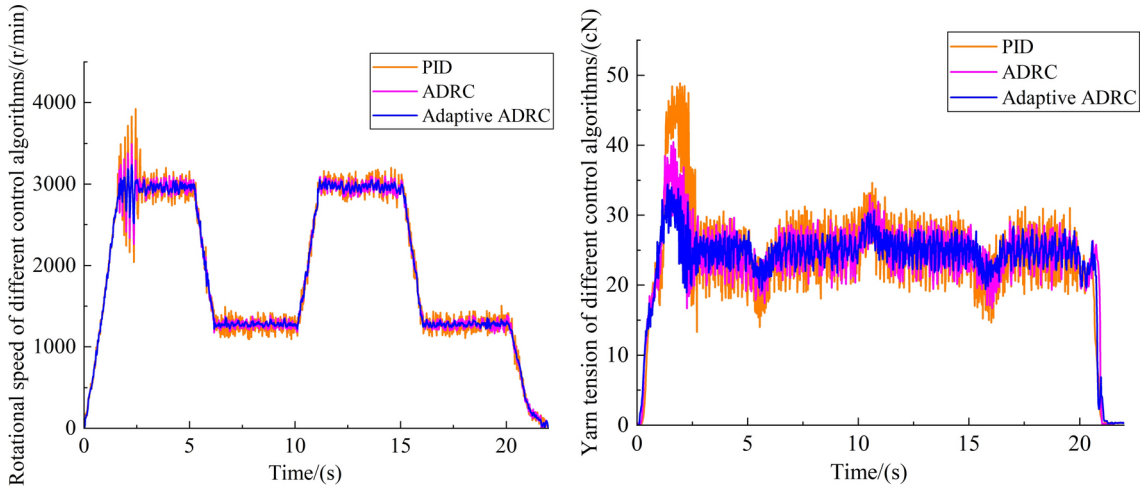

(a) Yarn feeder rotational speed curves **(b)** Yarn tension curves

Fig. 13. Experimental results of periodic adjustment of needle cylinder's rotational speed.

	PID		ADRC		Adaptive ADRC	
Tension stabilization phase	Mean error/cN	Standard deviation/cN	Mean error/cN	Standard deviation/cN	Mean error/cN	Standard deviation/cN
2975r/min	0.38	3.66	0.29	2.65	0.058	1.63
1275r/min	− 0.26	3.11	− 0.12	2.23	− 0.055	1.43

Table 10. Tension results of stabilization phase under periodic adjustment of target rotational speed of needle cylinder.

	Rotational speed increases by 68r/min		Rotational speed reduces by 68r/min	
Tension fluctuation phase	Overshoot/%	Response time/s	Undershoot/%	Response time/s
PID	38.6	1.68	43.9	1.80
ADRC	30.8	1.17	33.0	1.24
Adaptive ADRC	22.6	0.75	21.9	0.81

Table 11. Tension results of fluctuation phase under periodic adjustment of target rotational speed of needle cylinder.

As illustrated in Fig. 14, the experimental data from the three control algorithms clearly demonstrate that the adaptive ADRC algorithm outperforms the PID and ADRC algorithms in terms of tension control precision and response speed. Specifically, for tension control precision, the 95% confidence interval for the mean maximum tension deviation of the adaptive ADRC algorithm is [5.42, 5.59]cN, which is 47.7% and 31.6% lower than the corresponding values for the PID and ADRC algorithms, respectively (confidence level is 95% for all reported intervals). These results provide strong evidence of the adaptive ADRC algorithm's exceptional performance in reducing yarn tension fluctuations and enhancing control precision. Moreover, regarding response speed, the confidence interval for the mean response time of the adaptive ADRC algorithm is [0.775, 0.794] seconds, demonstrating a reduction of over 35% compared to the intervals of the PID and ADRC algorithms. These findings highlight the system's ability to improve tension control precision and response speed, ultimately enhancing product quality.

Verification experiment of yarn tension control performance under varying yarn types

To validate the tension control performance of the yarn delivery system under different yarn types, tests were conducted using common yarns in lingerie knitting, including cotton yarn, wool yarn, and spandex. The initial rotational speed of the needle cylinder simulation motor is set to 80r/min (corresponding to a yarn feed motor rotational speed of 2000r/min), and the initial yarn tension is set to 20cN. Yarn delivery experiments are performed for each of the three types of yarn. The tension curve data for each algorithm under different yarn types are shown in Fig. 15 and Table 12. Figure 16 presents the statistical results of the average mean deviation of tension and the average standard deviation of tension for controllers based on different algorithms, obtained through the repetition of the aforementioned experiments 200 times.

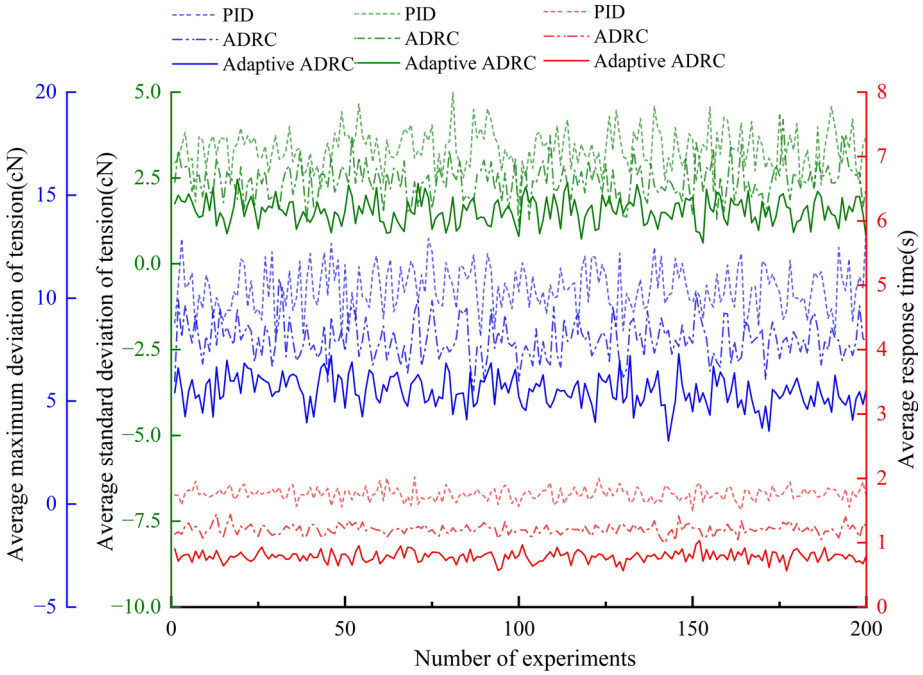

Fig. 14. Experimental results of various performance indexes of different algorithms in multiple rounds of variable target rotational speed experiment.

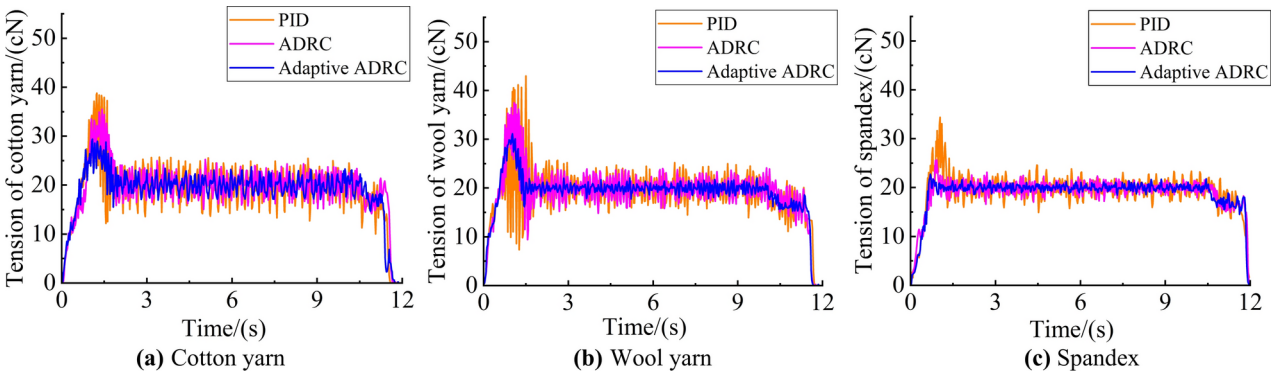

Fig. 15. Tension curves of different types of yarns.

	PID		ADRC		Adaptive ADRC	
Tension stabilization phase	Mean error/cN	Standard deviation/cN	Mean error/cN	Standard deviation /cN	Mean error/cN	Standard deviation /cN
Cotton yarn	0.18	2.72	0.13	2.08	0.04	1.56
Wool yarn	0.12	2.47	0.05	1.96	– 0.02	0.78
Spandex	0.03	1.66	0.02	1.03	0.01	0.57

Table 12. Results of real-time steady-state tension under conditions of different yarn types.

From Fig. 15a,b,c, it can be observed that stable yarn tension control is achieved for all three types of yarns, but there are significant differences in control performance. The maximum standard deviation for cotton yarn is 2.72cN, while for spandex, it is only 1.66cN. The tension fluctuation stability increases in the order of cotton yarn, wool yarn, and spandex, which is inversely related to the yarn's elasticity modulus, aligning with the yarn tension formation mechanism established earlier. Furthermore, the adaptive ADRC algorithm outperforms the other two algorithms in tension control for different yarns, with a reduction in mean error by more than 50% and an optimization in standard deviation by at least 25%. This demonstrates that the adaptive ADRC controller can achieve stable yarn control in knitting underwear machines using various types of yarn.

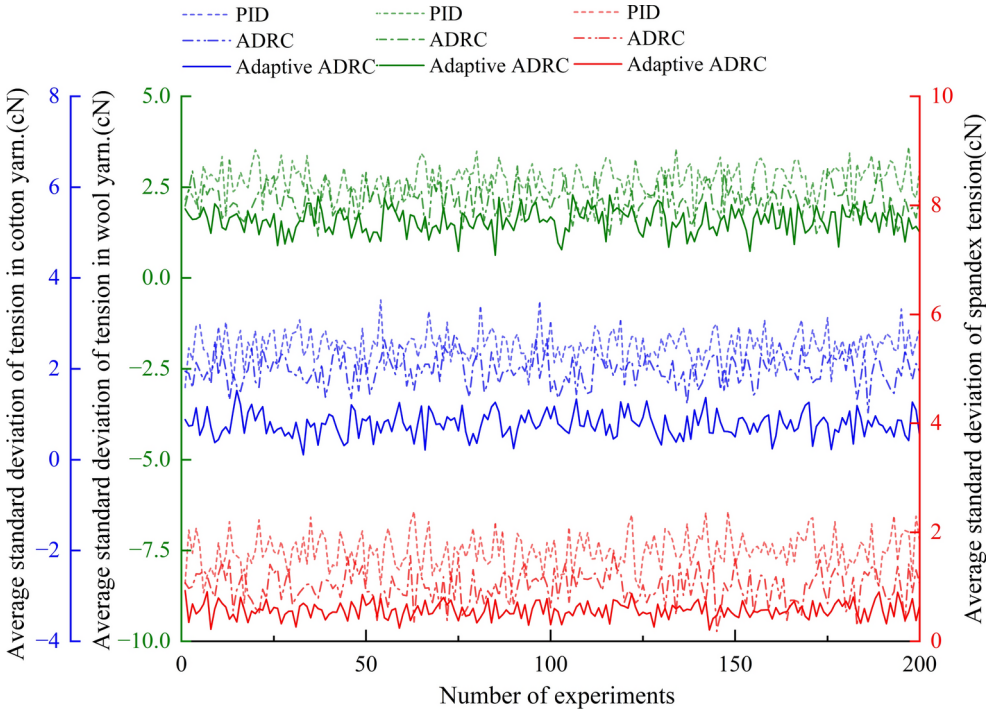

Fig. 16. Experimental results of various performance indicators of different algorithms in multiple rounds of experiments with different types of yarns.

Through statistical analysis of the data presented in Fig. 16, it is evident that the adaptive ADRC algorithm demonstrates significant advantages over both the PID algorithm and the ADRC algorithm. Specifically, the confidence interval for the average standard deviation of tension in the adaptive ADRC algorithm, which is [1.54,1.62] cN, is reduced by 41.5% compared to the PID algorithm on cotton yarn and by approximately 23.3% compared to the ADRC algorithm. On wool yarn, this metric is decreased by 68.3% and 58.8% compared to the PID algorithm and ADRC algorithm, respectively. On spandex, it decreases by 65.5% and 43.9%, respectively. These quantitative data indicate that the adaptive ADRC algorithm excels in reducing yarn tension fluctuations, and this advantage remains consistent across various types of yarns. Therefore, the adaptive ADRC controller is capable of achieving stable yarn control under different yarn working conditions in knitting underwear machines.

Conclusion

To address the issues of low-tension tracking accuracy and large tension fluctuation errors in the current yarn feeding control systems of knitting lingerie machines, this paper proposes a yarn tension control system based on the adaptive Active Disturbance Rejection Control (ADRC) algorithm. The system is integrated with a permanent magnet synchronous motor (PMSM) vector control system to achieve stable yarn tension control during the operation of the knitting lingerie machine.

Simulation and experimental data demonstrate that when the yarn target tension and needle cylinder motor speed undergo dynamic adjustments, the adaptive ADRC control algorithm significantly outperforms both the PID algorithm and the traditional ADRC algorithm in terms of yarn tension control. Under different operating conditions, the yarn tension response time of the control system based on the adaptive ADRC algorithm is reduced by over 35% compared to that of both the PID algorithm and the conventional ADRC algorithm, and the yarn tension fluctuation is reduced by more than 33%, and the maximum deviation suppression during yarn tension abrupt changes is enhanced by at least 30%. indicating that the adaptive ADRC algorithm offers superior dynamic tracking accuracy. This validates the excellent performance of the proposed control algorithm.

By adopting this control system, it is possible to improve the precision of yarn tension control while reducing the response time during sudden changes in the target tension. This enhances the stability of yarn tension in the operation of knitting underwear machines and accelerates the system's response speed, effectively reducing the defect rate of fabric caused by issues related to elasticity and density. Moreover, it provides a significant approach to further improving the control precision and stability of textile machinery, offering promising application prospects in the field of textile machinery.

Data availability

To data that support the findings of this study are available from the corresponding author upon reasonable request.

Received: 22 December 2024; Accepted: 17 March 2025
Published online: 21 March 2025

References

1. Syed, U., Jhatial, A. R. & Peerzada, H. M. Influence of warp yarn tension on cotton woven fabric structures. *J. Mehran Univ. Res. J. Eng. Technol.* **32**(1), 125–132 (2013).
2. Jin, R. Niu, Q. Research on textile defects detection based on improved generative adversarial network. J. J. Eng. Fibers Fabr. 17 (2022).
3. Šajn, D., Geršak, J. & Flajs, R. Prediction of stress relaxation of fabrics with increased elasticity. *J. Text. Res. J.* **76**(10), 742–750 (2006).
4. Geršak, J. Study of relationship between fabric elastic potential and garment appearance quality. *J. Int. J. Cloth. Sci. Technol.* **16**(1/2), 238–251 (2004).
5. Ronggen, Z., Pei, F. & Chongchang, Y. A study on the unwinding tension control of an elastic yarn. *J. Text. Res. J.* **92**(23–24), 4587–4595 (2002).
6. Zhao, B., Cong, H. & Wu, G. Construction and system realization of the yarn tension model of fully fashioned flat knitting fabric. *J. Text. Res. J.* **91**(11–12), 1380–1388 (2021).
7. Feng, J. Q. et al. Research and application of a new constant tension control device of the carbon fiber warping machine. *J. Adv. Mater. Res.* **846–847**, 40–43 (2013).
8. Xiao, Y. et al. Optimal analysis and application of the warp tension control system for a rapier loom. *J. Text. Res. J.* **92**(7–8), 1213–1225 (2022).
9. Li, Y., Li, H. M. & Li, Y. Schemes selection of yarn tension detection and control based on fuzzy multiple attribute group decision making. *J. Adv. Mater. Res.* **694**, 2829–2834 (2013).
10. Wang, C. C. & Zhao, X. H. The control algorithm research of yarn tension for winding machine based on grey prediction model. *J. Appl. Mech. Mater.* **3009**(519–520), 1305–1308 (2014).
11. Hua, Z. et al. Tension control of a yarn winding system based on the nonlinear active disturbance-rejection control algorithm. *J. Text. Res. J.* **92**(23–24), 5049–5065 (2022).
12. Baoping, Z. & Gaoming, J. Design of yarn tension self-adaptive control system on warp knitting machine. *J. Text. Inst.* **115**(2), 173–187 (2024).
13. Chen, P., Cheng, Y., Yuan, Y. & Hua, L. Sliding mode tension control for the yarn winding process with extended state observer. *Trans. Inst. Meas. Control* **47**(2), 291–303. https://doi.org/10.1177/01423312241242514 (2024).
14. Nosraty, H. et al. Influence of controlled weft yarn tension of a single nozzle air-jet loom on the physical properties of the fabric. *J. Text. Res. J.* **76**(8), 637–645 (2006).
15. Gang, L., Chuanfang, X. & Longda, W. Modified ADRC design of permanent magnet synchronous motor based on improved memetic algorithm. *J. Sens.* **23**(7), 3621 (2023).
16. Zhao, L. & Shi, Y. Disturbance suppression of gimbal servo motor based on improved ADRC and ISMC Method. *J. Electr. Eng. Technol.* **19**, 4285–4295 (2024).
17. Li, C. et al. An efficient tracking differentiator based active disturbance rejection control for flight environment simulation system. *J. Aerosp. Sci. Technol.* **155**(P1), 109578–109578 (2024).
18. Liang, T. et al. Speed tracking and synchronization of a multi-motor system based on fuzzy ADRC and enhanced adjacent coupling scheme. *J. Complex.* **2018**(2018), 5632939,1-5632939,16 (2018).
19. Lelisa, W. et al. A comparative study of fuzzy SMC with adaptive fuzzy PID for sensorless speed control of six-phase induction motor. *J. Energies* **15**(21), 8183–8183 (2022).
20. Ying, Q. et al. Sliding-mode anti-disturbance speed control of permanent magnet synchronous motor based on an advanced reaching law. *J. ISA Trans.* **139**, 436–447 (2023).
21. Ma, S. et al. Sliding-mode control of linear induction motor based on exponential reaching law. *J. Electron.* **13**(12), 2352–2352 (2024).
22. Lai, C. K. & Shyu, K. K. A novel motor drive design for incremental motion system via sliding-mode control method. *IEEE Trans. Ind. Electron.* **52**, 499–507 (2005).
23. Wang, A. et al. Design of sliding mode controller for servo feed system based on generalized extended state observer with reinforcement learning. *J. Sci. Rep.* **14**(1), 24976–24976 (2024).
24. Li, Z. et al. Application research of fuzzy PID control optimized by genetic algorithm in medium and low speed maglev train charger. *J. IEEE Access.* **9**, 152131–152139 (2021).
25. Yin, H. et al. Research on brushless DC motor control system based on fuzzy parameter adaptive PI algorithm. J. AIP Advances, **10**(2020) .
26. Baoye, S., Yihui, X. & Lin, X. Design of fuzzy PI controller for brushless DC motor based on PSO–GSA algorithm. *J. Syst. Sci. Control Eng.* **8**(1), 67–77 (2020).
27. Asgharnia, A., Shahnazi, R. & Jamali, A. Performance and robustness of optimal fractional fuzzy PID controllers for pitch control of a wind turbine using chaotic optimization algorithms. *J. ISA Trans.* **79**, 27–44 (2018).
28. Song, K. et al. Online self-adaptive proportional-integral-derivative control for brushless DC motor based on variable universe fuzzy inference system optimized by genetic algorithm. *J. Proc. Inst. Mech. Eng. Part C J. Mech. Eng. Sci.* **236**(10), 5127–5142 (2022).
29. Zhang, B. et al. Fuzzy PID control of permanent magnet synchronous motor electric steering engine by improved beetle antennae search algorithm. *J. Sci. Rep.* **14**(1), 2898–2898 (2024).
30. Signe, R. K. & Motto, F. B. Fuzzy-PID controller based sliding-mode for suppressing low frequency oscillations of the synchronous generator. *Heliyon* **10**(15), e35035. https://doi.org/10.1016/j.heliyon.2024.e35035 (2024).

Acknowledgements

The authors are thankful to National Key R&D Program of China for funding this work through the Researchers Supporting Project (SO2023YFB3200093). The authors are also thankful to Zhejiang Provincial Key Laboratory of Modern Textile Equip-ment and Technology of Zhejiang Sci-Tech University for partial support.

Author contributions

L.P. wrote the main manuscript and found out the results. X. X. wrote the graphical description and completed data curation. L.W. used the software and formal analysis of the manuscript. All authors reviewed the manuscript.

Funding

This research was funded by National Key R&D Program of China (SO2023YFB3200093) and Zhejiang Province "High-Level Talent Special Support Program" Leading Talent in Technological Innovation (2023R5212) and

General scientific research project of Zhejiang Provincial Department of Education (y202456420) and Key Cultivation Project for the Integration of Science and Education at Zhejiang Polytechnic University of Mechanical and Electrical Engineering (A-0271–24-209).

Competing interests
The authors declare no competing interests.

Additional information
Correspondence and requests for materials should be addressed to L.W.

Reprints and permissions information is available at www.nature.com/reprints.

Publisher's note Springer Nature remains neutral with regard to jurisdictional claims in published maps and institutional affiliations.